

Studies on the phase behavior and solubilization of the microemulsion formed by surfactant-like ionic liquids with ϵ - β -fish-like phase diagram

Chengkuan Qin · Jinling Chai · Jingfei Chen · Yan Xia · Xiaoying Yu · Jing Liu

Received: 23 July 2007 / Revised: 21 October 2007 / Accepted: 29 November 2007 / Published online: 8 January 2008
© Springer-Verlag 2007

Abstract The phase behavior and the solubilization of the microemulsion systems surfactant-like ionic liquids 1-hexadecyl-3-methylimidazolium bromide ($C_{16}\text{mimBr}$), 1-tetradecyl-3-methylimidazolium bromide ($C_{14}\text{mimBr}$), or 1-dodecyl-3-methylimidazolium bromide ($C_{12}\text{mimBr}$)/alcohol/alkane/brine have been studied with ϵ - β -fish-like phase diagram method at 40 °C and an oil-to-water mass ratio of 1:1. From the ϵ - β -fish-like phase diagram, the physico-chemical parameters, such as the mass fraction of alcohol in the hydrophile-lipophile-balanced interfacial layer (A^S), and the solubilities of ionic liquid (S^O) and alcohol (A^O) in alkane phase, were calculated. The solubilization of the microemulsion system has been discussed based on the ϵ - β -fish-like phase diagram. The smaller the oil molecule, the longer the alcohol chain length, and the larger the NaCl concentration in water, the larger the solubilization of the microemulsion system. In this paper, the solubilization of the microemulsion stabilized by both $C_{12}\text{mimBr}$ and sodium dodecyl sulfonate (sodium dodecyl sulfate) was also investigated with the ϵ - β -fish-like phase diagram. The unequimolar composite of anionic and cationic surfactants can avoid the sedimentation aroused by the strong electrostatic attraction, and an obvious synergism effect in solubilization was obtained.

Keywords Phase behavior · Fish-like phase diagram · Solubilization · Ionic liquid · Microemulsion

Introduction

Microemulsions are thermodynamically stable mixtures of two immiscible solvents stabilized by surfactants. Because of their unique properties, such as ultralow interfacial tension, large interfacial area, and the ability to solubilize otherwise immiscible liquids, microemulsions have been widely used in various fields such as tertiary oil recovery, separation [1], pharmaceuticals [2], nanoparticle synthesis [3–6], chemical engineering [7], and so on.

Ionic liquids (ILs), a class of molten organic salts at or near room temperature, have attracted much attention in recent years. ILs have unique chemical and physical properties such as negligible vapor pressure, thermal stability, non-flammability, high ionic conductivity, and a possible wide electrochemical window. These ideal properties of ILs qualify them as alternatives to conventional organic solvents used in organic or inorganic synthesis [8, 9], catalysis [10], chemical separation [11, 12], and electrochemical application [13]. Recent developments involve their use for biopolymers [14], molecular self-assemblies [15, 16], and synthesis of novel nanostructures [17, 18]. To explore and enhance the applications of ILs, the incorporation of surfactants with/within ILs has been investigated in micelle, vesicles, emulsions, and liquid crystallines [19–22]. ILs, based on the 1-alkyl-3-methylimidazolium cation ($C_n\text{mim}$), possess an inherent amphiphilicity; the surface adsorption [23] of a series of $C_n\text{mim-X}$ ($n=4, 8, 12$; $X=\text{PF}_6^-, \text{BF}_4^-, \text{Cl}^-, \text{Br}^-$) and the dynamic surface tension of $C_4\text{mim-PF}_6^-$ [24] have been reported.

Recently, using ILs instead of water or oil to prepare ILs microemulsion is an interesting research field. Microemulsion composed of hydrophilic IL, $C_4\text{mim-BF}_4$, has been prepared and characterized. The experiment

C. Qin · J. Chai (✉) · J. Chen · Y. Xia · X. Yu · J. Liu
Department of Chemistry, Shandong Normal University,
Jinan 250014, People's Republic of China
e-mail: jlchai99@163.com

shows that the microemulsion droplet has the same shape as “classic” water-in-oil (W/O) microemulsion [25–29]. Using lipophilic IL, $C_4\text{mim-PF}_6$, to form microemulsion has also been reported, and the water-in-ionic liquid (W/IL), bicontinuous, and ionic liquid-in-water (IL/W) microregions of the Triton X-100/water/ $C_4\text{mim-PF}_6$ ternary system microemulsions were identified by cyclic voltammetry method [30]. Yan and Texer reported that ILs can be used as surfactants to stabilize microemulsions, and studied the polymerization in these microemulsions [31].

Kunieda et al. developed the HLB plane method (δ - γ -fish-like phase diagram) and used to investigate the phase behavior of microemulsion systems [32–36]. Our research group studied the phase behavior of microemulsion systems with Winsor type, δ - γ - and ε - β -fish-like phase diagrams, respectively [37–40]. A ε - β -fish-like phase diagram method was presented by our research group [38, 39] and used to calculate the parameters and discuss the solubilization power of the microemulsion systems precisely.

In this paper, three kinds of surfactant-like ionic liquids, 1-alkyl-3-methylimidazolium bromide ($C_{12}\text{mimBr}$, $C_{14}\text{mimBr}$, and $C_{16}\text{mimBr}$), were synthesized by us and used as surfactants to prepare microemulsions with different alcohols (*n*-butanol, *n*-pentanol, *n*-hexanol), and different alkanes (*n*-hexane, *n*-octane, *n*-decane). The phase behavior and the solubilization of the microemulsion system were characterized using the ε - β -fish-like phase diagram. According to our knowledge, such a study on the middle-phase microemulsion of surfactant-like ionic liquids was modestly reported in the past.

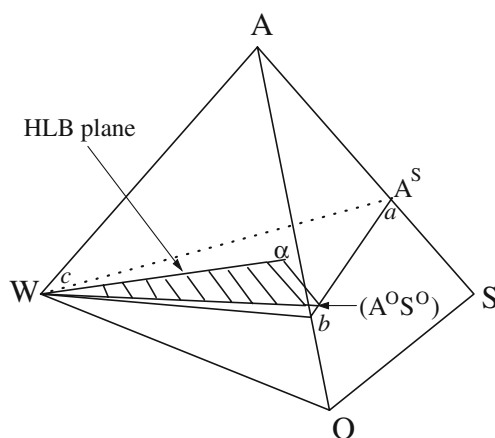
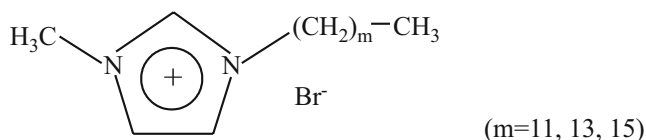


Fig. 1 Sketch of the HLB plane in a tetrahedral phase diagram for quaternary system surfactant (S)/alcohol (A)/oil (O)/water (W). The area with hatching means a three-phase triangle in the midst of a three-phase region. A^O the solubility of alcohol in oil, S^O the solubility of surfactant in oil, A^S the mass fraction of alcohol in the interfacial layer

Experimental section

Materials and apparatus

1-Hexadecyl-3-methylimidazolium bromide ($C_{16}\text{mimBr}$) was synthesized by the reaction of 1-methylimidazole with an equimolar amount of 1-bromohexadecane in acetonitrile at 80 °C under a nitrogen atmosphere for 2 days. 1-Tetradecyl-3-methylimidazolium bromide ($C_{14}\text{mimBr}$) was synthesized by the reaction of 1-methylimidazole with an equimolar amount of 1-bromotetradecane in acetonitrile at 80 °C under a nitrogen atmosphere for 3 days, and 1-dodecyl-3-methylimidazolium bromide ($C_{12}\text{mimBr}$) was synthesized by the reaction of 1-methylimidazole with an equimolar amount of 1-bromododecane in toluene at 70–75 °C under a nitrogen atmosphere for 3 days. Further purification and characterization of the three products were conducted based on the instructions found in the literature [41]. The products obtained were white crystal solids with the melting points 39.6 °C ($C_{12}\text{mimBr}$), 48.4 °C ($C_{14}\text{mimBr}$), and 53.8 °C ($C_{16}\text{mimBr}$), respectively. The purity of all the ionic liquids synthesized was examined, and no surface tension minimum was found in the surface tension curve. The structure of surfactant-like ionic liquids $C_{m+1}\text{mimBr}$ is as follows:



n-Butanol, *n*-pentanol, *n*-hexanol, *n*-hexane, and *n*-octane (analytically pure) were purchased from Sinopharm Chem-

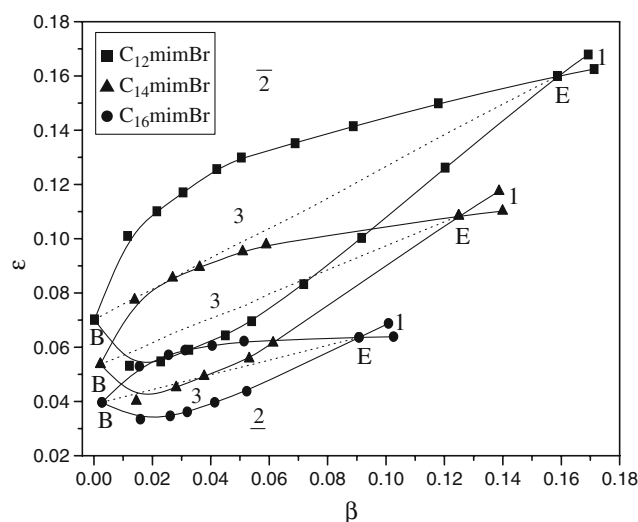


Fig. 2 ε - β -fish-like phase diagram for the quaternary system surfactant-like ionic liquids/*n*-butanol/*n*-octane/brine (5%NaCl) at 40 °C and $\alpha=0.5$

Table 1 Physical parameters of β_B , ε_B , β_E , ε_E , S^O , A^O , A^S , C_S , C_A , and A_{eff}^S for the quaternary system surfactant-like ionic liquids/*n*-butanol/*n*-octane/brine (5%NaCl)

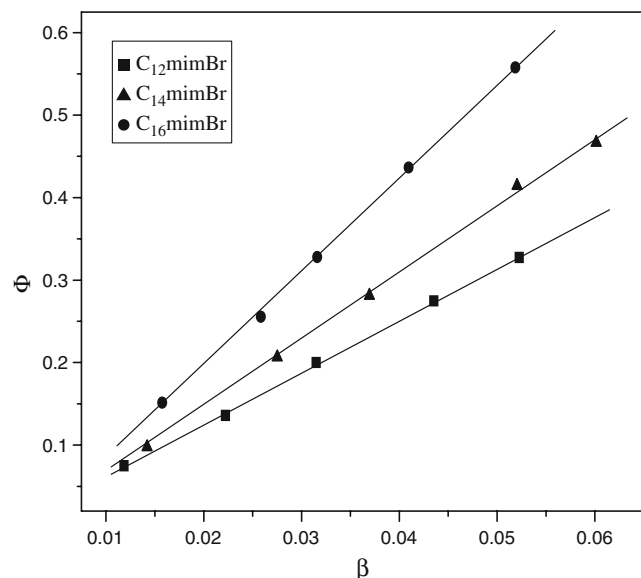
Surfactant	β_B	ε_B	β_E	ε_E	S^O	A^O	A^S	C_S	C_A	A_{eff}^S
C ₁₆ mimBr	0.00277	0.0397	0.0908	0.0637	0.00532	0.0761	0.2447	0.0884	0.0286	0.2447
C ₁₄ mimBr	0.0022	0.0537	0.1249	0.1084	0.00417	0.1017	0.3448	0.1231	0.0648	0.3448
C ₁₂ mimBr	0.000167	0.0702	0.1587	0.1599	0.00031	0.1311	0.4062	0.1586	0.1085	0.4063

ical Reagent Co., Ltd, Shanghai, China and used without further purification. *n*-Decane (99%) was purchased from Alfa Aesar Johnson Matthey, USA and used without further purification. Sodium dodecyl sulfonate (AS; analytically pure) and sodium dodecyl sulfate (SDS; analytically pure) were purchased from Beijing Chemical Reagent Co., Ltd, Beijing, China. AS and SDS were recrystallized with alcohol/acetone mixture twice. Water was doubly distilled.

FA1104 electronic analytical balance (Shanghai, China) and DF-101S constant temperature magnetic mixer (Jiangsu, China) were used in this study.

Methods

ILs microemulsions were prepared by weighing the surfactant-like ionic liquids into Teflon-sealed glass tubes and diluting to the desired concentrations with NaCl aqueous solution. Then, the oil was weighed and placed into the tubes. A 1:1 ratio of water to oil was preferred. The amount of alcohols (*n*-butanol, *n*-pentanol, *n*-hexanol) was varied monotonically, while ionic liquid concentrations were fixed at different values. All samples were allowed to equilibrate at 40 ± 0.1 °C in a water bath for 1 week. Phase equilibrium was determined by visual observations, and the volumes of all phases were recorded.

**Fig. 3** Volume fraction, Φ , of the middle phase at the mid-point of the middle-phase region as a function of β

For the quaternary system of surfactant (*S*)/alcohol (*A*)/oil (*O*)/water (*W*), the following composition variables are defined as the mass fraction of oil in oil and water mixtures, $\alpha = O/(W + O)$, the mass fraction of surfactant in the total system, $\beta = S/(S + A + O + W)$, the mass fraction of alcohol in the total system, $\varepsilon = A/(S + A + O + W)$, the mass fraction of surfactant and alcohol in the total system, $\gamma = (S + A)/(S + A + O + W)$, and the mass fraction of alcohol in the surfactant and alcohol mixture, $\delta = A/(S + A)$. $\bar{\delta}$ and $\bar{\varepsilon}$ are the mid-point values of δ and ε in the middle-phase region for the given values of γ and β , respectively.

If temperature and pressure are constant, and α is held at 0.50, β is plotted horizontally, and ε plotted vertically, a two-dimensional ε - β -fish-like phase diagram can be obtained.

Results and discussion

The ε - β -fish-like phase diagram

The phase diagram of a quaternary system at constant temperature and pressure can be plotted in a tetrahedron (Fig. 1), a particular three-phase tie triangle (α - b - c) through

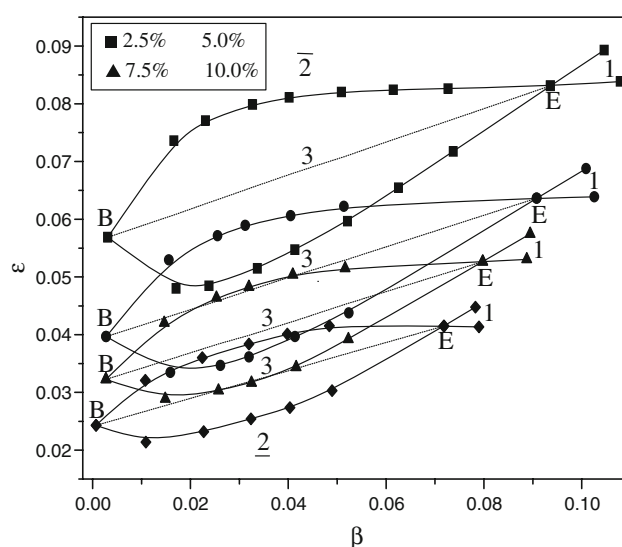
**Fig. 4** ε - β -fish-like phase diagram for the quaternary system C₁₆mimBr/*n*-butanol/*n*-octane/brine with different NaCl concentrations at 40 °C and $\alpha=0.5$

Table 2 Physical parameters of β_B , ϵ_B , β_E , ϵ_E , S^O , A^O , A^S , C_S , C_A , and A_{eff}^S for the quaternary system $C_{16}\text{mimBr}/n\text{-butanol}/n\text{-octane}/\text{brine}$ with different NaCl concentrations

wt.%	β_B	ϵ_B	β_E	ϵ_E	S^O	A^O	A^S	C_S	C_A	A_{eff}^S
2.5%	0.00309	0.0569	0.0936	0.0831	0.00583	0.1073	0.2682	0.0909	0.0333	0.2681
5.0%	0.00277	0.0397	0.0908	0.0636	0.00532	0.0761	0.2447	0.0884	0.0286	0.2447
7.5%	0.00271	0.0323	0.0797	0.0526	0.00524	0.0623	0.2341	0.0773	0.0236	0.2341
10.0%	0.000692	0.0243	0.0718	0.0415	0.00135	0.0474	0.2140	0.0712	0.0194	0.2140

such a tetrahedron is obtained; points α , b , and c denote the composition of the microemulsion in the midst of the Winsor III region, oil and water phases, respectively. In this tie triangle, the middle-phase microemulsion solubilizes equal amount of oil and water. This section is called a hydrophile–lipophile-balanced plane (HLB plane).

The ϵ – β -fish-like phase diagram for surfactant-like ionic liquids $C_{16}\text{mimBr}$ ($C_{14}\text{mimBr}$, $C_{12}\text{mimBr}$)/ n -butanol/ n -octane/brine (5%NaCl) system was shown in Fig. 2. It can be seen from Fig. 2 that increasing ϵ at constant β causes a series of phase inversions Winsor I(2)→III(3)→II(2). The “fish head” is downwards, and the “fish tail” is upwards.

Calculation of some physical parameters

In Fig. 2, the midst line of the middle-phase region locates in the HLB plane. The hydrophile–lipophile property of the interfacial layer in the quaternary system is just balanced in the midst line of the middle-phase region. The composition of the microemulsion in the midst line of the Winsor III region obeys the ϵ – β HLB plane equation, which is put forward based on the δ – γ HLB plane equation [32]. For a quaternary system, the middle-phase region obeys [32]

$$\bar{\delta} = A^S + F\alpha \left(\frac{1}{\gamma} - 1 \right) \quad (1)$$

In Eq. 1, $\bar{\delta}$ and γ were defined as follows

$$\bar{\delta} = \frac{A}{A+S} = \frac{\bar{\epsilon}}{\beta + \bar{\epsilon}}; \gamma = \frac{S+A}{W+O+S+A} = \beta + \bar{\epsilon} \quad (2)$$

Substituting from Eq. 2 into Eq. 1, the ϵ – β HLB plane equation was obtained as Eq. 3

$$\bar{\epsilon} = \frac{A^S - F\alpha}{1 - A^S + F\alpha} \beta + \frac{F\alpha}{1 - A^S + F\alpha}; \quad (3)$$

$$F = \frac{A^O S^S - S^O A^S}{1 - S^O - A^O}$$

Where S^S and A^S are the mass fractions of surfactant and alcohol in the interfacial layer ($A^S + S^S = 1$); S^O and A^O are the solubilities of surfactant and alcohol in oil, respectively. A plot of $\bar{\epsilon}$ vs β is a straight line (the broken line in Fig. 2).

If the slope and intercept of Eq. 3 are K and I , respectively, then A^S can be obtained by

$$A^S = \frac{K + I}{1 + K} \quad (4)$$

The experimental values of A^S can be calculated from Eq. 4 and are shown in Table 1.

Equation 1 contains a reciprocal term ($1/\gamma$), and the relating midst line of the middle-phase region in δ – γ -fish-like phase diagram is a steep curve; it is difficult to draw out the midst line precisely and calculate the composition of the interfacial layer accurately, especially when the γ values are very small. In addition, the abscissas of the end point E (γ_E) of the middle-phase represent the mass fractions of the total amounts of surfactant and alcohol, lacking clear physical meanings. The ϵ – β -fish-like phase diagram (Fig. 2) and Eq. 3 overcome all the disadvantages of the δ – γ -fish-like phase diagram, especially, the coordinates of the end point E (β_E , ϵ_E) show the solubilization power of the microemulsion system more clearly.

The “fish head” (point B) in Fig. 2 indicates the formation of middle-phase microemulsion, and the “fish

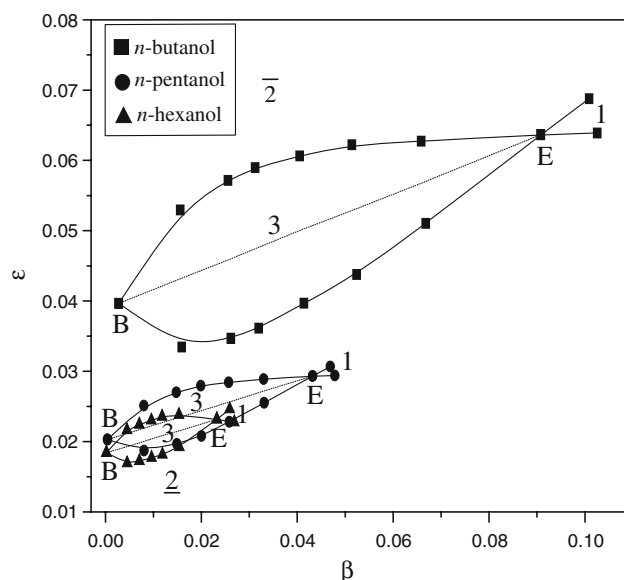
**Fig. 5** ϵ – β -fish-like phase diagram for the quaternary system $C_{16}\text{mimBr}/n\text{-octane}/\text{alcohol}/\text{brine}$ (5%NaCl) at 40 °C and $\alpha=0.5$

Table 3 Physical parameters of β_B , ε_B , β_E , ε_E , S^O , A^O , A^S , C_S , C_A , and A_{eff}^S for the quaternary system $C_{16}\text{mimBr}/n\text{-octane}/\text{alcohol}$ (n -butanol, n -pentanol, n -hexanol)/brine (5%NaCl)

Alcohol	β_B	ε_B	β_E	ε_E	S^O	A^O	A^S	C_S	C_A	A_{eff}^S
n -Butanol	0.00277	0.0397	0.0908	0.0637	0.00532	0.0761	0.2447	0.0884	0.0286	0.2447
n -Pentanol	0.00043	0.0203	0.0432	0.0293	0.00084	0.0398	0.1908	0.0428	0.0101	0.1908
n -Hexanol	0.00018	0.0184	0.0232	0.0232	0.00036	0.0362	0.1868	0.0230	0.0053	0.1868

tail" (point E) indicates the disappearing of the three-phase microemulsion, and β_E and ε_E reveal the minimum concentration of surfactant-like ionic liquids and alcohol for getting a single-phase microemulsion, while the ratio of water to oil is 1. The smaller the β_E and ε_E values, the larger the solubilization of the system.

The volume fraction, Φ , of the middle phase at the midst line (Fig. 3) was measured for a series of β values and plotted as a function of β . Extrapolation of this linear function to $\Phi=0$ and $\Phi=1$, the abscissas of the starting point B (β_B) and the end point E (β_E) were obtained, respectively. The values of ε_B and ε_E at these two points were calculated by applying ε - β HLB plane equation (Eq. 3). The values of β_B , ε_B , β_E , and ε_E are listed in Table 1.

The solubilities of surfactant (S^O) and alcohol (A^O) in oil phases can be calculated by the following equation

$$S^O = \frac{\beta_B}{\alpha + (1 - \alpha)(\beta_B + \varepsilon_B)}$$

$$A^O = \frac{\varepsilon_B}{\alpha + (1 - \alpha)(\beta_B + \varepsilon_B)}$$
(5)

The values of S^O and A^O are all listed in Table 1.

In Table 1, S^O is much smaller than A^O , which shows that mainly short-chain alcohols dissolve in oil phase, and the solubility of the surfactant in oil phase can be neglected.

The mass fraction of surfactant (C_S) and alcohol (C_A) contained in the balanced interfacial layer in the total system can be calculated by using the simple-mass-balanced equation.

$$C_S = \beta_E - \frac{\beta_B(1 - \beta_E - \varepsilon_E)}{(1 - \beta_B - \varepsilon_B)}$$

$$C_A = \varepsilon_E - \frac{\varepsilon_B(1 - \beta_E - \varepsilon_E)}{(1 - \beta_B - \varepsilon_B)}$$
(6)

Equation 6 can be used to calculate the relative proportions of surfactant and alcohol in the interfacial layer not only for point E, but also for any other point along the trajectory β , ε of the mid-points of the three-phase region. Thus, the mass fraction of alcohol in the interfacial layer can also be expressed

$$A_{\text{eff}}^S = \frac{C_A}{C_A + C_S}$$
(7)

The values of C_S , C_A , and A_{eff}^S are listed together in Table 1.

It can be found in Table 1 that according to the values of β_E and ε_E , the solubilization power of the microemulsion is

$C_{16}\text{mimBr} > C_{14}\text{mimBr} > C_{12}\text{mimBr}$. The values of C_S and β_E are approximately equal, which demonstrates that the surfactant almost all assemble in the hydrophile-lipophile-balanced interfacial layer. C_A is obviously smaller than ε_E , which shows that the lipophilic n -butanol is easier to dissolve in oil than surfactant-like ionic liquid molecules. From Fig. 3, it can be found that the volume fraction of middle phase at the mid-point of the middle-phase region at the same β , $C_{16}\text{mimBr}$ is obviously larger than the other two kinds of surfactant-like ionic liquids, and it also indicates that the solubilization power of the surfactant-like ionic liquid is $C_{16}\text{mimBr} > C_{14}\text{mimBr} > C_{12}\text{mimBr}$.

Effect of NaCl concentration on the ε - β -fish-like phase diagram

The effect of NaCl concentration on the ε - β -fish-like phase diagram has been investigated. Fig. 4 shows the ε - β -fish-like phase diagrams for quaternary system $C_{16}\text{mimBr}/n\text{-butanol}/n\text{-octane}/\text{brine}$ with different NaCl concentrations. The physical parameters were listed in Table 2.

From Fig. 4 and Table 2, it can be seen that NaCl concentration has a great influence on the ε - β -fish-like phase diagram. With the increase in NaCl concentration in aqueous phase, β_E and ε_E decrease notably. It can be

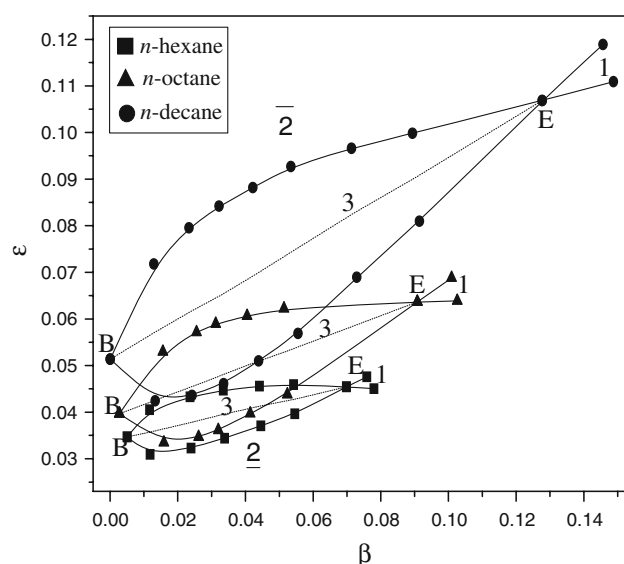
**Fig. 6** ε - β -fish-like phase diagram for the quaternary system $C_{16}\text{mimBr}/n\text{-butanol}/n\text{-alkane}/\text{brine}$ (5%NaCl) at 40 °C and $\alpha=0.5$

Table 4 Physical parameters of β_B , ϵ_B , β_E , ϵ_E , S^O , A^O , A^S , C_S , C_A , and A_{eff}^S for the quaternary system $C_{16}\text{mimBr}/n\text{-butanol}/n\text{-hexane}$ ($n\text{-octane}$, $n\text{-decane}$)/brine (5%NaCl)

$n\text{-Alkane}$	β_B	ϵ_B	β_E	ϵ_E	S^O	A^O	A^S	C_S	C_A	A_{eff}^S
$n\text{-Hexane}$	0.00507	0.0347	0.0699	0.0455	0.00975	0.0667	0.1717	0.0652	0.0135	0.1716
$n\text{-Octane}$	0.00277	0.0397	0.0908	0.0637	0.00532	0.0761	0.2447	0.0884	0.0286	0.2447
$n\text{-Decane}$	0.000078	0.0514	0.1277	0.1068	0.00015	0.0977	0.3387	0.1276	0.0654	0.3389

explained that the ionization of the cationic surfactant makes the microemulsion droplets charge positively. If inorganic salts such as NaCl dissolve into the water, the counterion (Cl^-) of the salt will compress the electrical double layer of the microemulsion droplets [42], which increases the ability for microemulsion to aggregate. The O/W microemulsion easily changes into the W/O-type microemulsion via bicontinuous microemulsion. With the increase in salinity, the solubilization power of microemulsion increases.

Effect of alcohols on the ϵ - β -fish-like phase diagram

The effect of alcohols with different carbon chain lengths on the ϵ - β -fish-like phase diagrams for quaternary system $C_{16}\text{mimBr}/n\text{-octane}/\text{alcohol}/\text{brine}$ (5%NaCl) was shown in Fig. 5, and the physical parameters of these systems were listed in Table 3.

It can be found in Table 3 that the longer the carbon chains of alcohol molecules, the smaller the values of β_E and ϵ_E , that is, the larger the solubilization power of the microemulsion. Alcohol molecules can change the hydrophilicity of the amphiphilic layer. The alcohols with longer carbon chains have higher efficiency to change the hydro-

philicity, making the amphiphilic layer more lipophilic, or less hydrophilic, so less alcohol is needed to balance the hydrophile-lipophile property of the amphiphile layer. The values of C_S and β_E are approximately equal, but C_A is smaller than ϵ_E , which shows that all alcohols dissolve in oil besides in the interfacial layer.

Effect of alkane on the ϵ - β -fish-like phase diagram

The effect of alkanes with different carbon chain lengths on the ϵ - β -fish-like phase diagrams for quaternary systems $C_{16}\text{mimBr}/n\text{-octane}/n\text{-butanol}/\text{brine}$ (5%NaCl) was shown in Fig. 6, and the physical parameters of these systems were listed in Table 4.

It can be found in Table 4 that the shorter the carbon chains of alkane molecules, the smaller the values of β_E and ϵ_E , that is, the larger the solubilization power of the microemulsion. The order of the solubilization power is $n\text{-hexane} > n\text{-octane} > n\text{-decane}$. It is because the alkane with shorter carbon chain length can easily penetrate the barriers of the microemulsion droplets formed by the oriented surfactant and alcohol molecules, which makes the mean curvature of the amphiphilic film turned toward oil.

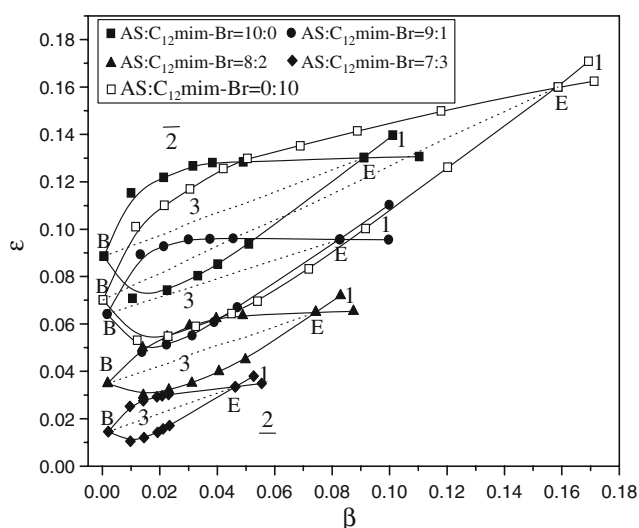
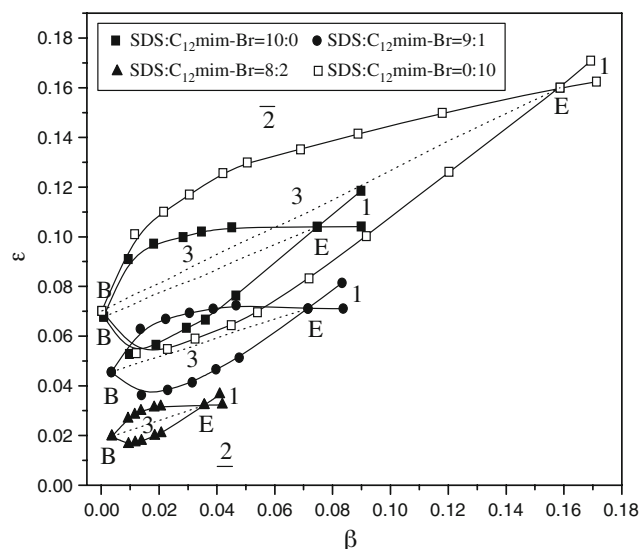
**Fig. 7** Influence of the mole ratio of AS/ $C_{12}\text{mimBr}$ on the ϵ - β -fish-like phase diagrams of AS- $C_{12}\text{mimBr}/n\text{-octane}/n\text{-butanol}/\text{brine}$ (5% NaCl) microemulsion systems at 40 °C and $\alpha=0.5$ **Fig. 8** Influence of the mole ratio of SDS/ $C_{12}\text{mimBr}$ on the ϵ - β -fish-like phase diagrams of SDS- $C_{12}\text{mimBr}/n\text{-octane}/n\text{-butanol}/\text{brine}$ (5% NaCl) microemulsion systems at 40 °C and $\alpha=0.5$

Table 5 Physical parameters of β_B , ϵ_B , β_E , ϵ_E , S^O , A^O , A^S , C_S , C_A , and A_{eff}^S for the quaternary system AS–C₁₂mimBr/*n*-butanol/*n*-octane/brine (5%NaCl)

Ratio ^a	β_B	ϵ_B	β_E	ϵ_E	S^O	A^O	A^S	C_S	C_A	A_{eff}^S
10:0	0.00054	0.0886	0.0911	0.1302	0.00099	0.1627	0.3755	0.0907	0.0545	0.3754
9:1	0.00168	0.0642	0.0827	0.0957	0.00315	0.1205	0.3256	0.0812	0.0392	0.3256
8:2	0.00182	0.0349	0.0743	0.0649	0.00352	0.0673	0.3171	0.0726	0.0337	0.3171
7:3	0.00206	0.0146	0.0463	0.0335	0.00405	0.0288	0.3086	0.0444	0.0198	0.3086
0:10	0.000166	0.0702	0.1587	0.1599	0.00031	0.1311	0.4063	0.1586	0.1085	0.4063

^a The mole ratio of AS to C₁₂mimBr

Effect of anionic and cationic surfactants composite on the ϵ – β -fish-like phase diagram

Composite surfactants with unequimolar anionic and cationic surfactants usually demonstrate high synergistic effect. In this study, sodium dodecyl sulfonate (AS)–C₁₂mimBr mixture system and sodium dodecyl sulfate (SDS)–C₁₂mimBr mixture system with different mole ratios were investigated. The ϵ – β -fish-like phase diagrams for the quaternary systems AS–C₁₂mimBr (SDS–C₁₂mimBr)/*n*-octane/*n*-butanol/brine (5%NaCl) were shown in Figs. 7 and 8, and the physical parameters of these systems were listed in Tables 5 and 6, respectively.

From Figs. 7 and 8, and Tables 5 and 6, it can be seen that the phase diagrams of the composite surfactant systems move to the lower position, and ϵ_E and β_E decrease dramatically, and the solubilization of the composite surfactant microemulsion system was enhanced obviously. The experiment shows that the mole fraction of C₁₂mimBr in AS/C₁₂mimBr and SDS/C₁₂mimBr composite systems should be less than 0.40 and 0.30, respectively, or else, sedimentation would appear.

The unequimolar ratios of anionic and cationic surfactants can avoid the formation of sedimentation aroused by a strong electrostatic effect and obtain distinct synergism effect in phase behavior and solubilization. The synergism effect between anionic surfactant and cationic surfactant roots in the strong electrostatic attraction among the positive and negative ions of the surfactants in the interfacial layer. This kind of attraction makes the surfactant

molecules easy to be adsorbed more compactly in the interfacial layer, so this kind of anionic and cationic surfactant composite system possesses excellent and attractive solubilization power.

Conclusions

The phase behavior of middle-phase microemulsion for the quaternary system surfactant-like ionic liquids/alcohol/*n*-alkane/brine was investigated based on the ϵ – β -fish-like phase diagram at 40 °C and $\alpha=0.5$. The physicochemical parameters for the quaternary system were determined. The microemulsion solubilization power for the surfactant-like ionic liquids is C₁₆mimBr>C₁₄mimBr>C₁₂mimBr.

In the microemulsion system, surfactant molecules mainly dissolve in the interfacial layer, however, alcohol dissolves in oil besides in the interfacial layer.

Salts can enhance the solubilization power of the microemulsion due to the compression of the counterions of the salt to the electrical double layer of the microemulsion droplets.

The longer the alcohol chain length, the larger the solubilization power of the microemulsion. It is also found that the shorter the oil's carbon chain length, the easier the microemulsion inversion Winsor I→III→II.

The phase behavior of the unequimolar AS/C₁₂mimBr and SDS/C₁₂mimBr composite microemulsion systems were also investigated with the ϵ – β -fish-like phase diagram, and found that an obvious synergism effect in solubilization power exists.

Table 6 Physical parameters of β_B , ϵ_B , β_E , ϵ_E , S^O , A^O , A^S , C_S , C_A , and A_{eff}^S for the quaternary system SDS–C₁₂mimBr/*n*-butanol/*n*-octane/brine (5%NaCl)

Ratio ^a	β_B	ϵ_B	β_E	ϵ_E	S^O	A^O	A^S	C_S	C_A	A_{eff}^S
10:0	0.00086	0.0678	0.0747	0.1040	0.0016	0.1269	0.3743	0.0739	0.0442	0.3743
9:1	0.00351	0.0456	0.0715	0.0711	0.0067	0.0869	0.3053	0.0684	0.0300	0.3053
8:2	0.00364	0.0196	0.0356	0.0322	0.0071	0.0383	0.2951	0.0322	0.0135	0.2951
0:10	0.000166	0.0702	0.1587	0.1599	0.00031	0.1311	0.4063	0.1586	0.1085	0.4063

^a The mole ratio of SDS to C₁₂mimBr

Acknowledgment This work was supported by the Natural Science Foundation of Shandong Province of China (Grant No.: Y2003B01).

References

1. Firman P, Kahlweit M (1996) *J Phys Chem* 100:1216
2. Acosta EJ, Nguyen T, Witthayapanyanon A, Harwell JH, Sabatini DA (2005) *Environ Sci Technol* 39:1275
3. Yoon B, Wai CM (2005) *J Am Chem Soc* 127:17174
4. Khomane RB, Manna A, Mandale AB, Kulkarni BD (2002) *Langmuir* 18:8237
5. Xing Y, Li M, Davis SA, Mann S (2006) *J Phys Chem B* 110:1111
6. Ethayaraja M, Bandyopadhyaya R (2006) *J Am Chem Soc* 128:17102
7. Candau F, Zekhini Z, Heatley F (1986) *Macromolecules* 19:1895
8. Dyson PJ (2002) *Transit Met Chem* 27:353
9. Ding S, Radosz M, Shen Y (2005) *Macromolecules* 38:5921
10. Sheldon R (2001) *Chem Commun* 23:2399
11. Huddleston JG, Willauer HD, Swatoski RP, Visser AE, Rogers RD (1998) *Chem Commun* 16:1765
12. Zhao H, Xia SQ, Ma PS (2005) *J Chem Technol Biotechnol* 80:1089
13. Endres F, Bukowski M, Hempel-mann R, Natter H (2003) *Angew Chem Int Ed* 42:3428
14. Swatoski RP, Spear SK, Holbrey JD, Rogers RD (2002) *J Am Chem Soc* 124:4974
15. Araos MU, Warr GG (2005) *J Phys Chem B* 109:14275
16. He Y, Li Z, Simone P, Lodge TP (2006) *J Am Chem Soc* 128:2745
17. Canongia Lopes JNA, Padua AAH (2006) *J Phys Chem B* 110:3330
18. Zhu H, Huang JF, Pan Z, Dai S (2006) *Chem Mater* 18:4473
19. Fletcher KA, Pandey S (2004) *Langmuir* 20:33
20. Merrigan TL, Bates ED, Dorman SC, Davis JH (2000) *Chem Commun* 20:2051
21. Firestone MA, Dzielawa JA, Zapol P, Curtiss LA, Seifert S, Dietz ML (2002) *Langmuir* 18:7258
22. Wang ZN, Liu F, Gao YA, Zhuang WC, Xu LM, Han BX, Li GZ, Zhang GY (2005) *Langmuir* 21:4931
23. Law G, Watson PR (2001) *Langmuir* 17:6138
24. Gao YA, Wang ZN, Zhang J, Hou WG, Li GZ, Han BX, Lv FF, Zhang GY (2005) *Chin Chem Lett* 16:963
25. Gao HX, Li JC, Han BX, Chen WN, Zhang JL, Zhang R, Yan DD (2004) *Phys Chem Chem Phys* 6:2914
26. Eastoe J, Gold S, Rogers SE, Paul A, Welton T, Heenan RK, Grillo I (2005) *J Am Chem Soc* 127:7302
27. Chakrabarty D, Seth D, Chakraborty A, Sarkar N (2005) *J Phys Chem B* 109:5753
28. Gao YA, Zhang J, Xu HY, Zhao XY, Zheng LQ, Li XW, Yu L (2006) *Chem Phys Chem* 7:1554
29. Li N, Gao YA, Zheng LQ, Zhang J, Yu L, Li XW (2007) *Langmuir* 23:1091
30. Gao YA, Han SB, Han BX, Li GZ, Shen D, Li ZH, Du JM, Hou WG, Zhang GY (2005) *Langmuir* 21:5681
31. Yan F, Texter J (2006) *Chem Commun* 25:2696
32. Kunieda H, Shinoda K (1985) *J Colloid Interface Sci* 107:107
33. Kunieda H, Hanno K, Yamaguchi S, Shinoda K (1985) *J Colloid Interface Sci* 107:129
34. Muto M, Naito N, Kunieda H (1994) *Yukagaku (J Jpn Oil Chem Soc)* 43:502
35. Kunieda H, Nakano A, Pes MA (1995) *Langmuir* 11:3302
36. Yamaguchi S, Kunieda H (1997) *Langmuir* 13:6995
37. Chai JL, Wu CJ, Li GZ, Zhang GY (2003) *Chin J Chem* 21:25
38. Chai JL, Zhao JR, Gao YH, Yang XD, Wu CJ (2007) *Colloids Surf A* 302:31
39. Yang XD, Gao YH, Chai JL, Wu CJ, Li GZ (2007) *Chin J Chem* 25:53
40. Chai JL, Yang XD, Gao YH, Wu CJ (2007) *Polish J Chem* 81:547
41. Dupont J, Consorti CS, Suarez PAZ, Souza RF (1999) *Org Synth* 79:236
42. Bourrel M, Schechter RS (1988) In: *Microemulsion and related systems: Formulation, solvency, and physical properties*, Chapter 7. Marcel Dekker, New York and Basel